

# Seismic interferometry facilitating the imaging of shallow seismic reflectors hidden beneath surface waves

Jianhuan Liu\*, Ranajit Ghose and Deyan Draganov. Delft University of Technology

## Summary

High-resolution reflection seismics can be very helpful in subsurface imaging and monitoring in urban environments and in archaeological sites. An obstacle that hinders the success of high-resolution reflection seismic imaging of the very shallow targets is the presence of source-generated surface waves at soil-covered sites and surface waves generated by other anthropogenic sources, e.g., traffic and construction activities in the vicinity of the seismic line. Both of these can hide the very shallow reflection events. We have developed new schemes involving seismic interferometry (SI) to retrieve both source-coherent (and/or source-incoherent) surface waves part of data. The retrieved surface waves are then adaptively subtracted from the raw data, thereby exposing hidden reflections. We illustrate results on both synthetic and field seismic data. We show that artefacts caused by stacking the surface-wave noise are greatly reduced, and that reflectors, especially at very shallow depth, can be much better imaged and interpreted.

## Introduction

High-resolution reflection seismics is one of the few options to achieve the target resolution of the shallow subsurface in an urban setting. However, many investigated sites are characterized by soils overlying consolidated bedrock. Seismic data acquired at such sites exhibits strong surface waves hiding the very shallow reflections. Applying muting or spatial filtering to suppress the surface waves damages or completely eliminates the masked reflections. To preserve and reveal the very shallow reflections, we apply seismic interferometry (SI) and adaptive subtraction (AS) to reduce the masking surface waves.

Another typical and strong source of noise is human activities in the vicinity of the investigation sites, like traffic, construction works, and industrial activities. Such (source-incoherent) noise would give rise to linear/quasi-linear horizontal or dipping strong surface-wave arrivals in the raw field data, masking most of the very shallow reflections. In this research, we develop processing schemes also to suppress the source-incoherent noise based again on SI and AS.

## Methodology

SI refers to the retrieval of the full Green's function between two receivers by crosscorrelating and integrating of wavefields observed at these receivers from a boundary of

sources (Wapenaar and Fokkema, 2006). When the sources are located along the surface of the earth, the retrieved results are dominated by surface waves (Halliday *et al.*, 2007). Because of this, we make use of SI to retrieve dominant surface waves, and the retrieved surface-wave energy is then adaptively subtracted from the data. Using the model in Figure 1, we illustrate these steps in Figure 2 using synthetic data.

Figure 2a is a synthetic shot gather from a source located at 14 m in the horizontal direction at the surface. To retrieve a virtual common-source gather (CSG), we sort all the data into common-receiver gathers (CRGs). We then crosscorrelate CRG for a chosen virtual-source position (e.g., at 14 m) with another CRGs and stack the correlated traces. We repeat this correlation and summation for all other CRGs. This results in the virtual CSG as shown in Figure 2b. Comparing Figure 2a and Figure 2b, we can see that the dominant surface waves in Figure 2a are retrieved well in Figure 2b, as expected, while retrieved reflections are suppressed. This retrieved surface waves are then adaptively subtracted from Figure 2a, which leads to the result shown in Figure 2c.

When conducting seismic surveys in urban settings, there are often other types of noise sources like ongoing construction activities and industrial work taking place around the survey line. The noise caused by these sources can be characterized by dipping linear moveout. To simulate this situation, we add surface waves with dipping moveout to the previously modeled data. In Figure 2d, we show an example of the resulting gather, the source being at 5 m. Figure 2e is the result from the application of SI on Figure 2d. We can see that dipping arrivals (blue arrows in Figure 2e) are retrieved at both causal and acausal time. To approximate the dipping arrivals in Figure 2d as good as possible, the retrieved dipping arrivals in Figure 2e are first extracted using a combination of linear move out correction (LMO), singular value decomposition (SVD) filtering, and inverse LMO. We then use the acausal part of these isolated dipping arrivals and shifted them to the position of the physical dipping arrivals in Figure 2d. The result is shown in Figure 2f. The inline surface wave is retrieved at the correct time, and hence need only be isolated by subtracting the full retrieved dipping arrivals (blue arrows in Figure 2e) from Figure 2e, which results in Figure 2g. These retrieved dominant arrivals (Figure 2f and Figure 2g) can now be adaptively subtracted from Figure 2d, giving Figure 2h.

## Seismic interferometry facilitating the imaging of shallow seismic reflectors

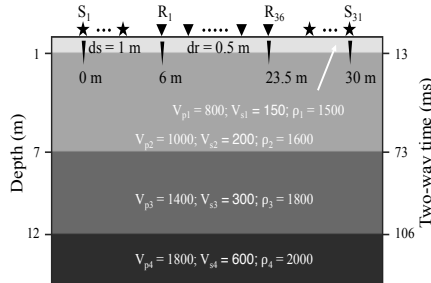


Figure 1: Geometry and model used to generate synthetic shot gathers via an elastic finite-difference modeling scheme (Thorbecke and Draganov 2011). The stars denote the sources, with a spacing of 1 m. The triangles represent the receivers; the interval is 0.5 m. The units for  $V_p$ ,  $V_s$ , and  $\rho$  are m/s, m/s, and kg/m<sup>3</sup>, respectively. The depth of each interface and its corresponding S-wave two-way time, are shown in left and right vertical axis, respectively.

In Figure 3, the effectiveness of SI+AS in the suppression of source-coherent and source-incoherent surface waves is compared with f-k filtering, and this effectiveness is further verified by a reference gather modeled without surface waves. Figure 3a is the shot gather as Figure 2a, Figure 3b and Figure 3c are the resulting gathers after f-k filtering and SI+AS, respectively. Comparing Figure 3a and Figure 3c, we can see that significant suppression of surface waves have been achieved using SI+AS, while the reflections are preserved well. F-k filtering (Figure 3b) is applied to reduce the surface waves, but it causes distortion (see red ellipse) to parts of the reflections. As is shown in Figure 3f, f-k filtering is even detrimental when it is used for suppressing the dipping arrivals in Figure 3e; it also causes total loss of informative reflections. However, such reflections are preserved in Figure 3g after SI+AS, with the source-coherent and source-incoherent surface waves greatly suppressed.

Figure 4 shows the stacked sections obtained from the data as in Figure 2a and Figure 2d after the application of f-k filtering and SI+AS. Comparing Figure 4b and Figure 4c, we can see that SI+AS performs better than f-k filtering in revealing true reflectors, because there are still some artifacts caused by stacking remaining surface waves (red ellipse in Figure 4b). For the case of data with also source-incoherent arrivals presented, f-k filtering (Figure 4e) fails, while the stacked section after SI+AS reduces significantly the artifacts present in Figure 4d and the reflectors can now be correctly imaged.

### Field-data example

In this high-resolution S-wave reflection field survey, the receiver line consisted of 120 horizontal-component geophones spaced at 0.25 m. The geophones were oriented

in the crossline direction. The receiver array was fixed during data collection, because of the limited available space in the survey area, which is a common constraint in urban settings. The source spacing was 1 m. Figure 5a shows a typical common-source gather, no reflections can be identified directly due to the heavy contamination by surface waves. As shown in Figure 5b, these surface waves are suppressed by f-k filtering, but this also causes many artifacts and substantial loss of useful reflections. However, in Figure 5c reflections (see red ellipse) are revealed due to the significant reduction of the surface waves by SI+AS. Figure 5d, 5e, 5f are the stacked sections from the raw data, data after f-k filtering, and data after SI+AS, respectively. In Figure 5f, shallow reflectors can now be clearly imaged around 100 ms and interpreted with a vertical resolution of less than 1 m (rms velocity used for stacking is 180 m/s), which is impossible in Figure 5d and Figure 5e.

### Conclusions

We developed new schemes for data-driven suppression of surface-wave noise that are commonly encountered during seismic surveys in urban settings or at archaeological sites. Using numerically modeled data, we showed how a combination of seismic interferometry and adaptive subtraction can significantly suppress inline (source-coherent) and crossline (source-incoherent) surface waves, which is ineffective by f-k filtering. Hence our schemes can improve significantly the imaging of shallow subsurface structures. We tested the effectiveness of our schemes by applying them to field seismic data collected in a very noisy area with the aim of imaging the shallow buried structures. By comparing the results from the original data with the results from the application of seismic interferometry and adaptive subtraction, we showed that artefacts, caused by stacking of surface-wave noise, are greatly reduced. As a result, reflectors, especially at very shallow depths, could be clearly imaged and interpreted with a vertical resolution of less than 1 m. Our schemes offer new options for high-resolution reflection seismic applied to urban geophysical applications.

### Acknowledgments

The research of J.L. is supported by China Scholarship Council. We would also like to thank Dominique Ngan-Tillard, Joeri Brackenhoff, and Jens van den Berg for their help during the field-data acquisition.

## Seismic interferometry facilitating the imaging of shallow seismic reflectors

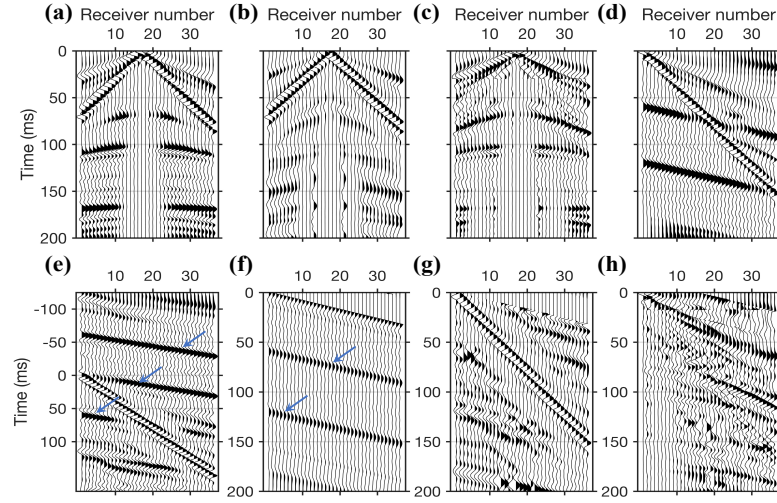


Figure 2: Steps for the implementation of SI+AS to suppress source-coherent surface waves: (a) A synthetic shot gather from the model shown in Figure 1; (b) retrieved surface waves from the data as in Figure 2a using SI; (c) result after AS of the data in Figure 2b from the data in Figure 2a. Steps for the implementation of SI+AS to reduce both source-coherent and dipping crossline surface waves: (d) A shot gather with source-coherent and source-incoherent surface waves present; (e) SI of the data as in Figure 2d; (f) retrieved dipping arrivals after shifting back to their physical position; (g) retrieved inline surface waves component; (h) AS of the result in Figure 2f and Figure 2g from Figure 2d. The blue arrows denote the retrieved dipping arrivals.

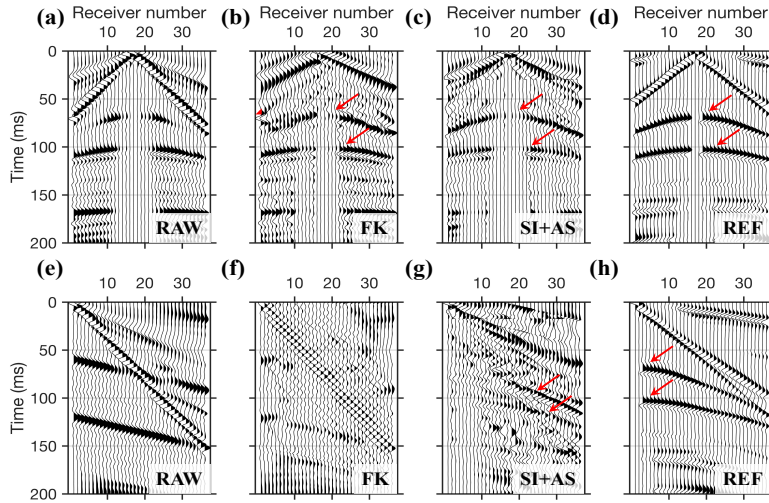


Figure 3: Comparison between shots gathers as in Figure 2a and Figure 2d after the application of f-k filtering and SI+AS: (a) Raw data as in Figure 2a; (b) result after f-k filtering; (c) result after SI+AS; (d) corresponding reference gather contains no surface waves, modeled by burying the source and receiver array in depth. (e) Raw gather as in Figure 2d; (f) result after f-k filtering; (g) result after SI+AS; (h) corresponding reference gather. The red arrows mark the primary S-wave reflections from the second and third interface of the model in Figure 1, respectively.

## Seismic interferometry facilitating the imaging of shallow seismic reflectors

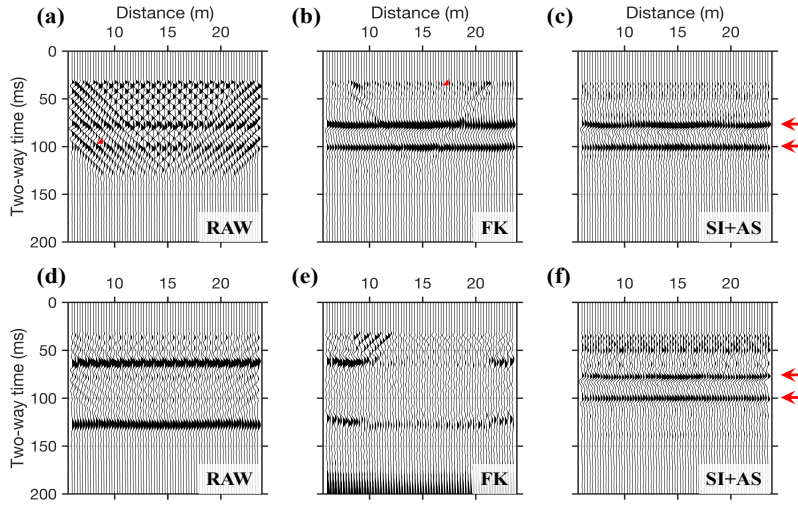


Figure 4: Comparison between stacked sections from shot gather as in Figure 2a and Figure 2d after the application of f-k filtering and SI+AS. (a) Stacked section from data as in Figure 2a without removal of surface waves; (b) stacked section after f-k filtering; (c) stacked section after SI+AS. (d) Stacked section from data as in Figure 2d without removal of surface waves; (e) stacked section after f-k filtering; (f) stacked section after SI+AS. The areas highlighted by red ellipses are caused by stacking of surface waves. Theoretical two-way time from the second and third reflectors of the model in Figure 1 are indicated by red arrows at the right side of the panels.

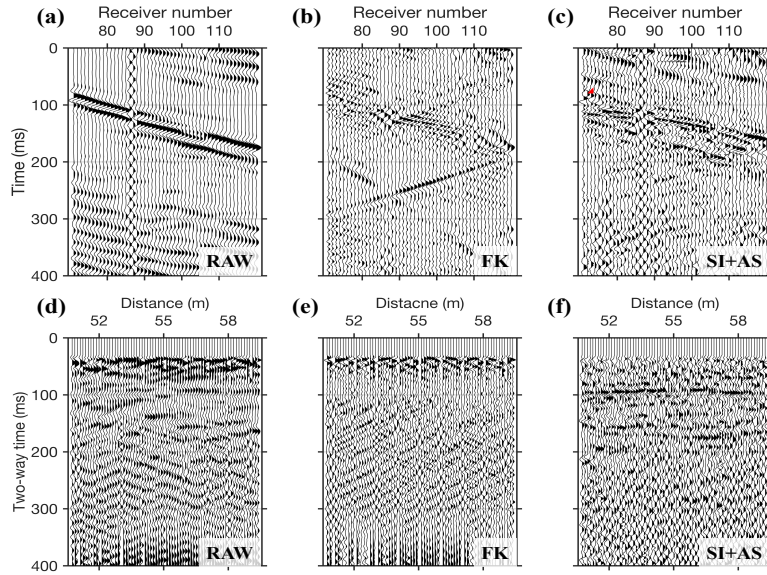


Figure 5: Comparison between field-data shot gathers: (a) A typical raw shot gather acquired in the field; (b) after f-k filtering; (c) after SI+AS, following the procedure as in Figure 2. Comparison between field-data stacked sections: (d) Using the raw field data; (e) using f-k filtered data; (f) using SI+AS data. The red ellipse marks the revealed shallow reflections via SI+AS.

## REFERENCES

- Halliday, D. F., A. Curtis, O. A. Robertsson, and D.-J. van Manen, 2007, Interferometric surface wave isolation and removal: *Geophysics*, **72**, no. 5, A69–A73, <https://doi.org/10.1190/1.2761967>.
- Thorbecke, J., and D. Draganov, 2011, Finite-difference modeling experiments for seismic interferometry: *Geophysics*, **76**, no. 6, H1–H18, <https://doi.org/10.1190/geo2010-0039.1>.
- Wapenaar, C. P. A., and J. Fokkema, 2006, Green's function representations for seismic interferometry: *Geophysics*, **71**, no. 4, S133–S146, <https://doi.org/10.1190/1.2213955>.